Soliton pairs in a fiber laser: from anomalous to normal average dispersion regime

Ph. Grelu, J. Béal and J. M. Soto-Crespo[*]

Laboratoire de Physique de l'Université de Bourgogne, Unité Mixte de Recherche 5027 du Centre National de Recherche Scientifique, B.P. 47870, 21078 Dijon, France
Philippe.Grelu@u-bourgogne.fr

[*]Permanent address: Instituto de Optica, Consejo Superior de Investigaciones Cientificas, Serrano 121, 28006 Madrid, Spain
jsoto@soliton.optica.csic.es

Abstract: We report the observation of self phase-locked pulse pairs in a stretched-pulse fiber laser operating in the normal path-averaged dispersion regime. Numerical simulations agree with our experimental results. More insight is provided with a numerical comparison between intracavity profiles of pulse pairs in anomalous and in normal dispersion regimes.

OCIS codes: (060.5530) Pulse propagation and solitons; (140.3510) Fiber lasers.

References and links

1. A. B. Grudinin, D. J. Richardson and D. N. Payne "Energy quantisation in figure eight fibre laser," Electron. Lett. **28**, 67-68 (1992).
2. M. J. Guy, D. U. Noske, and J. R. Taylor, "Generation of femtosecond soliton pulses by passive mode locking of an ytterbium-erbium figure-of-eight fiber laser," Opt. Lett **18,** 1447-1449 (1993).
3. A. B. Grudinin, D. J. Richardson and D. N. Payne, "Passive harmonic modelocking of a fiber soliton ring laser," Electron. Lett. **29**, 1860-1861 (1993).
4. D. Y. Tang, W. S. Man, H. Y. Tam and P. D. Drummond, "Observation of bound states of solitons in a passively mode-locked fiber laser," Phys. Rev. A **64**, 33814 (2001).
5. Ph. Grelu, F. Belhache, F. Gutty and J. M. Soto-Crespo, "Phase-locked soliton pairs in a stretched-pulse fiber laser" Opt. Lett. **27**, 966-968 (2002).
6. Ph. Grelu, F. Belhache, F. Gutty and J. M. Soto-Crespo, "Relative phase-locking of pulses in a passively mode-locked fiber laser," J. Opt. Soc. B **20**, 863-870 (2003).
7. N. N. Akhmediev, A. Ankiewicz, and J. M. Soto-Crespo, "Stable soliton pairs in optical transmission lines and fiber lasers", J. Opt. Soc. Am. B **15**, 515-523 (1998).
8. K. Tamura, E. P. Ippen, H. A. Haus, and L. E. Nelson, "77-fs pulse generation from a stretched-pulse mode-locked all-fiber ring laser," Opt. Lett. **18**, 1080-1082 (1993).

---

1. Introduction

In a passively mode-locked fiber laser, multiple pulsing is often observed when the pumping power exceeds a given threshold [1]. With operation in the anomalous dispersion regime, this threshold is quite low, and therefore up to tens of pulses may be observed to exist simultaneously in the cavity, as observed in early experiments [2]. This phenomenon seems attractive to seek for harmonic mode locking, which increases the cavity repetition rate. However, the stability of pulse-to-pulse separation is usually poor, due to the large spacing between subsequent pulses and the low level of stabilizing forces between these pulses [3]. Another possible behavior of the set of pulses is to bunch into a tight packet [1,2]. The bunched state may possess a remarkable degree of stability, as was stressed recently [4,5]. More precisely, it was shown that bunched pulses experience phase sensitive interactions,

similar to those of solitons, in a way that all the pulses may phase-lock to each other [6]. In the simplest case, which consists of two interacting pulses, it was shown that a soliton pair with a fixed separation and a relative phase around ±90° could form [5], as predicted theoretically in the frame of the complex quintic Ginzburg-Landau equation (CQGLE) [7]. This type of multisoliton state that arises in a dissipative system has distinct properties from the soliton states of a conservative system modeled for example with the usual nonlinear Schrödinger equation. In particular, for a given set of CQGLE parameters, a soliton pair can usually be described by two degrees of freedom: the relative phase between the two pulses and their distance of separation.

As the results of Ref. 7 were obtained in the anomalous case, we may wonder if phase-locked pulse pairs could form in the normal dispersion regime. In the present paper, we use a dispersion-managed stretched-pulse fiber ring laser operating in the regime of normal path-averaged dispersion [8]. We present the experimental observation of such phase-locked pulse pairs, and use a numerical propagation model of the laser to show the formation of a phase-locked pulse pair. A comparison between the bound pulse pair in normal dispersion and the soliton pair in anomalous dispersion is provided.

2. Experimental observation

The fiber ring laser setup is illustrated in Fig. 1. It comprises in series a 1400-ppm erbium-doped fiber (EDF) with normal dispersion [D = -40 (ps/nm)/km], a polarization insensitive coupler-isolator (WDM-IS) into which 980-nm pumping light is injected, a 10% output coupler, a length of SMF-28 fiber with anomalous dispersion [D = +16.5 (ps/nm)/km], and a 50-cm long open-air section containing wave plates and polarizing cubes. Due to nonlinear polarization evolution that takes place along with propagation in the fibers, the transmission through the polarizer P1 is intensity dependent, and an appropriate adjustment of the preceding wave plates triggers the mode-locking operation. The EDF length is here 1.9 m, while the choice of the SMF-28 length sets the path-averaged cavity dispersion either in an anomalous regime [D = +3.5(±0.5) (ps/nm)/km], or in normal regime [D = -2.5(±0.5) (ps/nm)/km]. The field can be monitored at three different output ports, labeled 1, 2 and 3 in Fig. 1. In this work we mainly use output 1, where a variable length of dispersion compensating fiber [DCF, D= -95.4 (ps/nm)/km] is spliced to the SMF-28 fiber output to compress the chirped pulses.
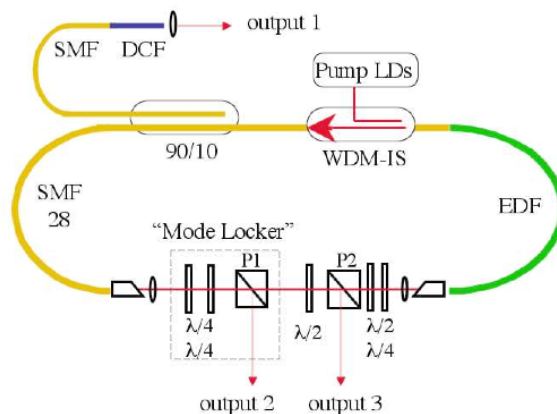

Fig. 1. Fiber ring laser experimental setup

The observation of soliton pairs in anomalous dispersion regime has been reported in Ref. 5. The features that follow were highlighted. The pair separation diminishes by steps with the decrease of the pumping power. This behavior has large hysteresis. For a moderate pumping power, in the 30 to 80 mW range, the intensity profile across each pulse is close to a sech^2

profile, and the phase relationship between the two solitons is measured to be around ±90°, in agreement with the analysis of Ref. 7. When the pumping power is higher than 80 mW, the optical spectrum widens, its envelope becomes slightly asymmetric, and the number of phase-locked pulses increases.

For operation into the normal dispersion regime, the required injected pumping power for mode locking is higher than 150 mW. Increasing the injected pumping power above 250 mW, we observe the formation of pulse pairs or triplets. According to the mode-locking settings and to the pumping power, several stable pulse-to-pulse separations can be observed, from less than 1 ps to more than 10 ps. We detail here the observation of a close pulse pair. Autocorrelation functions taken from outputs 2, 3 and from output 1 without DCF have the same, rather triangular shape (see Fig. 2(a)), whereas the recorded spectra all present the characteristic fringe pattern of a pulse pair.
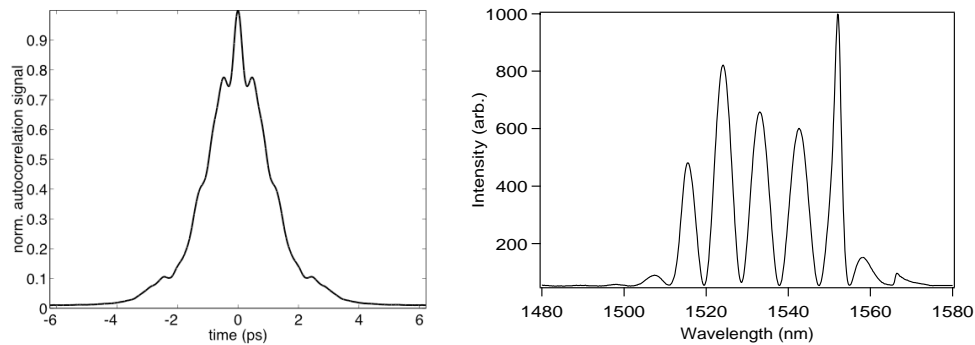

Fig. 2. (a) Autocorrelation function and (b) optical spectrum recorded at output 3.

The channeled spectrum structure, as shown in Fig. 2(b), has a high contrast which reveals a precise phase locking of the two pulses. According to the spectrum, we should find two pulses separated from around 850 fs. The spectral envelope has a width close to 35 nm, which means it could support 100 fs FWHM minimum pulse durations, assuming a gaussian pulse shape. Thus, Fig. 2(a) would be the autocorrelation of two close chirped pulses. In order to verify these, we spliced 52 cm of DCF to the end of SMF fiber of output 1. This DCF length compensates for the dispersion accumulated by the pulses in SMF fibers when traveling from the end of the EDF to the end of the SMF, after the 10% output coupler. Reducing gradually the DCF length, we obtained an optimum compression with a length of 36 cm, revealing the pulse pair structure. Corresponding autocorrelation trace and spectrum are displayed on Fig. 3.
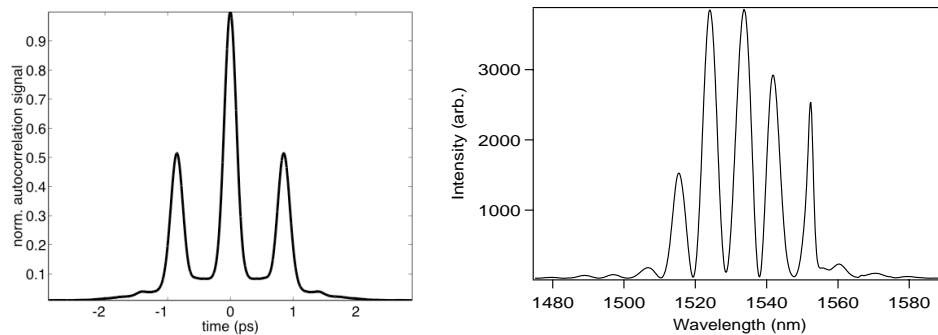

Fig. 3. (a) Compressed pulse pair and (b) optical spectrum recorded at output 1.

The autocorrelation trace is compatible with two pulses of same amplitude, separated by 870 fs. The main peak of the autocorrelation trace has a 230 fs FWHM, yielding 150 fs FWHM pulses. However, we remark the presence of small humps in the peaks sides, which means that the compressed pulse pair is not the superposition of two pure gaussian pulses.

As was stated, in the case of a single laser pulse [8], pulse shape is greatly affected by the change of the cavity path-averaged dispersion, from anomalous to normal regime. Spectral width and pulse energy are larger in the normal regime than in the anomalous regime. In our experiment, the pulse pair has an intracavity energy of 0.65 nJ, which is around 10 times the intracavity energy of soliton pairs reported in Ref. 5, for the anomalous regime. Along the propagation in the cavity, the pulse duration undergoes large changes due to the dispersion management effect. It is the so-called stretched-pulse operation of the fiber laser [8]. An estimate of the stretching factor is 10 in the present experiment, whereas it is less than 3 in the anomalous regime.

We have thus presented new experimental results showing that the normal dispersion regime is compatible with the formation of phase-locked states of two pulses. The numerical simulations that follow support these results.

3. Numerical simulation

We have developed the following propagation model for our fiber ring laser, which is sketched in Fig. 4, and is quite similar to the model described in Ref. 6. We were guided by the following principles: the model should include the physical effects needed to reproduce the main experimental behavior, while at same time contain a limited set of parameters. That is why all the elements in the open-air section of the real experiments are replaced in the model by a single polarizer whose axis may be oriented with an angle θ with respect to the fast axis of the slightly birefringent SMF fiber. For the sake of simplification and computational speed improvement, we also consider an "effective" fiber birefringence in the passive SMF fiber only.
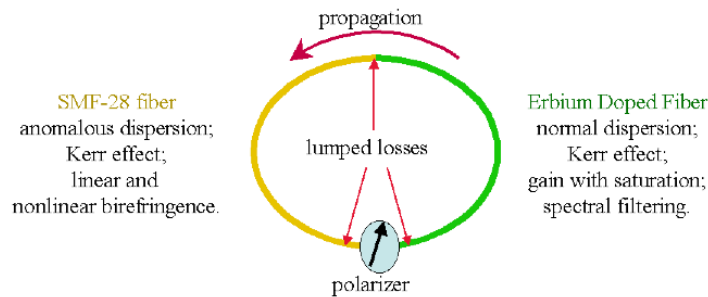

Fig. 4. Scheme of the numerical model

In the EDF, field propagation is modeled by the following scalar equation:

$$i\,E_z + \frac{D}{2}E_{tt} + \Gamma|E|^2 E = \frac{i\,g_0\,E}{1 + Q/Q_{sat}} + i\beta E_{tt} \tag{1}$$

where D is the dimensionless dispersion parameter ($D < 0$), and Γ the nonlinear coefficient. The small signal gain is g_0 and saturation energy is Q_{sat}, while Q represents the field energy at location z. The last term stands for the spectral filtering, which is mainly due to the limited bandwidth of the erbium gain.

At the input of the birefringent SMF fiber, a circularly polarized field is taken, to excite both principal axes, namely $(U,V) = (1,i)E/\sqrt{2}$. The propagation is modeled by the following two coupled equations:

$$i\,U_z + \gamma U + \frac{1}{2}U_{tt} + |U|^2 U + \frac{2}{3}|V|^2 U + \frac{1}{3}V^2 U^* = 0,$$

$$i\,V_z - \gamma V + \frac{1}{2}V_{tt} + |V|^2 V + \frac{2}{3}|U|^2 V + \frac{1}{3}U^2 V^* = 0. \tag{2}$$

After propagation in the SMF, the polarizer mixes the two components into a single component, namely $E = U\cos\theta + V\sin\theta$, and the latter is injected into the EDF until a stationary solution is found. For some sets of parameters, a two-pulse solution is formed, and we may follow its trajectory in the plane of pulse-to-pulse separation and phase difference. After each passage through the polarizer, the field is numerically analyzed to get separation and phase difference, which gives one point in this plane. Figure 5(a) presents several possible trajectories. Their starting points are marked by a green triangle. All blue trajectories are converging to one stable focus, which is marked as a red dot, whereas purple trajectories represent pulses which repell each other forever.
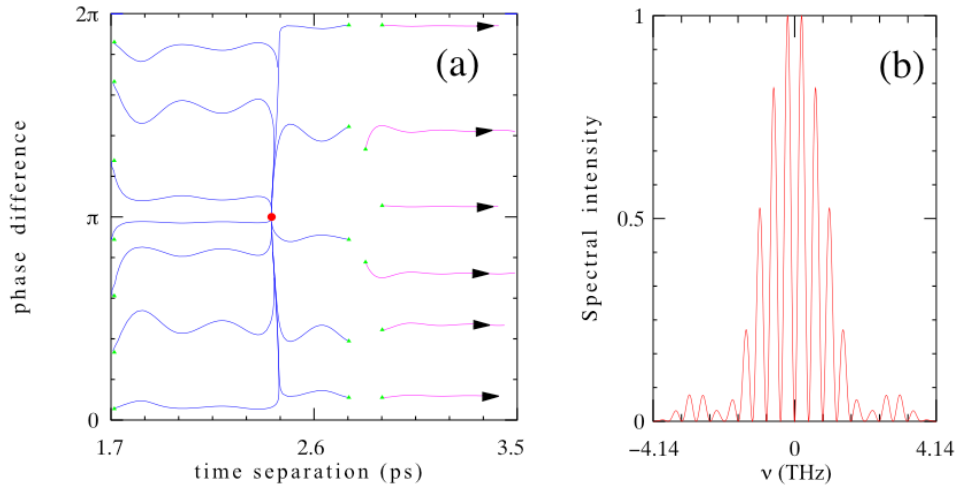

Fig. 5 (a) Trajectories of pulse pairs. The point denoted by a red dot acts as an attractor. (b) Optical spectrum corresponding to the stationary solution of the attractor, as taken after the polarizer. The parameters of the simulation are : L_{SMF}=3.6, L_{EDF}=1.88, Γ=3, γ=0.2, Q_{sat}=8, g_0=1.5, β=0.08, θ=142°.

In great contrast with the anomalous dispersion case studied in Ref. 6, where the soliton pairs spiralled towards a $\pm\pi/2$ phase-locked state, the dynamical evolution of pulse pairs in the present normal dispersion case is faster in terms of cavity round trips, and the attractor found is characterized by a π-phase difference. According to the values of the parameters used, one or several attractors may exist, and they are characterized by either a π or a zero phase relationship between the two pulses.

The optical spectrum of the stationary solution corresponding to the attractor of Fig. 5(a) is displayed on Fig. 5(b), showing common features with the experimental spectrum of Fig. 2(b), except for the envelope asymmetry of the experimental spectrum that is due to higher order effects not taken into account in the model. The experimental pulse pair is also closer than the numerical one, giving fewer fringes in its spectrum.

Figure 6(a) and Fig. 6(b), show the comparison of the intracavity propagation of the stationary states, in normal and anomalous path-averaged dispersion regimes, respectively. Both figures plot the square root of the optical intensity with respect to time, for increasing propagation distances in the cavity. The common feature is that the pulse-pair separation is kept constant, while each pulse undergoes large changes along the cavity round trip, due to gain and losses, dispersion and nonlinearity. However, shape changes are much less important

in the anomalous case : intracavity pulse duration varies from 250 to 600 fs, and the shape remains close to a slightly chirped sech^2 intensity profile. In the normal case, individual pulse shape and duration change considerably, and FWHM pulse durations vary from 100 fs to 1 ps. The magnitude of interaction due to a strong overlap in one part of the cavity in the normal case could also explain the change of dynamics near the attractor, as well as the π-phase relationship obtained instead of $\pi/2$ in the anomalous case.
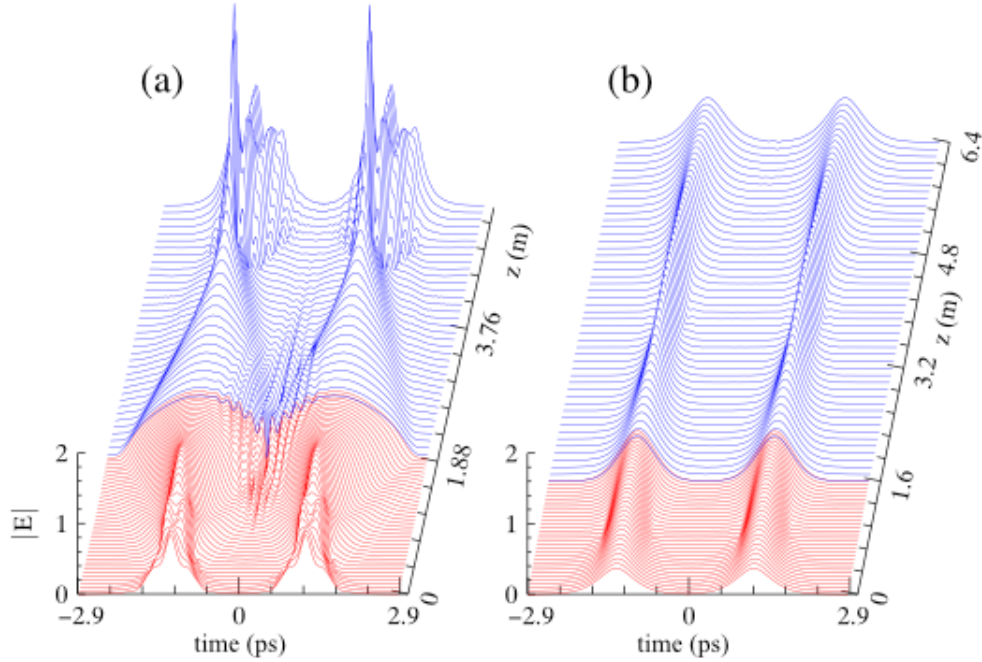

Fig. 6. Comparison of simulated field profiles along the dispersion-managed cavity. (a): in normal path-averaged dispersion regime, (b) in anomalous path-averaged dispersion regime. red colour is used for propagation in the EDF, whereas blue is for propagation in the SMF. The parameters used in (a) are the same as in Fig.5. The parameters used in (b) are: L_{EDF}=1.6 m, L_{SMF}=4.8 m , Γ=3, D=-2.3, γ=0.09, g_0=1.5, Q_{sat}=0.9, β=0.05, θ=70°. Time and distance are in real units, whereas one E-field unit is equal to 28 (Watt)$^{1/2}$.

4. Conclusion

We have discovered both experimentally and numerically the ability of a passively mode-locked stretched-pulse fiber laser to support stable phase-locked pulse pairs, in the normal average dispersion regime. Comparisons with phase-locked soliton pairs in the anomalous regime were provided. It revealed differences in the features of pulse pair attractors, namely in field profiles, interaction strength and phase relationships, as well as a common feature: during one cavity round trip, each pulse undergoes large changes, without affecting the self-phase locking of the two pulses. As the fiber laser cavity presents an analogy with an optical transmission line, our results could find application in the field of optical communications.

Acknowledgements